Sensors and Materials, Vol. 34, No. 11 (2022) 3989–4000
MYU Tokyo

S & M 3091

Estimation of Volume of Felled Chinese Fir Trees Using Unmanned Aerial Vehicle Oblique Photography

Jian-hua Hou,[1] Jian-ying Wang,[1] Xue-xin Ma,[1] and Dan Liang[2,3*]

[1]Natural Resources and Planning Bureau of Jingning She Autonomous County,
Jingning County, Zhejiang 323500, China
[2]Zhejiang Provincial Key Laboratory of Carbon Cycling in Forest Ecosystems and Carbon Sequestration,
Zhejiang A&F University, Hangzhou 311300, China
[3]College of Environmental and Resource Sciences, Zhejiang A&F University,
Hangzhou 311300, China

(Received June 20, 2022; accepted September, 13 2022)

Keywords: Chinese fir, cutting, volume, UAV remote sensing, tree height, root diameter

In forestry supervision, timely and accurate estimation of the felled tree volume is a very important task. Obtaining the felled tree volume by remote sensing using an unmanned aerial vehicle (UAV) is an effective means to reduce cost. Quantitative inversion of the felled tree volume of individual trees by visible light remote sensing using a UAV has major advantages but its accuracy is still a common concern in practice. The objective of this paper is to verify the feasibility and reliability of quantitative inversion of the felled tree volume by UAV visible light remote sensing. The proposed workflow is as follows. Firstly, raw images are obtained by UAV oblique photography and processed into a digital orthophoto map (DOM) and digital surface model (DSM) based on 3D reconstruction technology implemented in DJI Terra software. Secondly, based on before- and after-cutting DSM data, treetops are extracted using the conventional local maximum method, then are matched to the corresponding stump points. The tree height of the felled tree is estimated from the elevation difference between the treetop and the stump. Using the after-cutting DOM data, the root diameter and the geometric center of the felled tree are determined by the proposed circumcircle method. Thirdly, three regression models [estimated tree height and measured tree height, measured tree height and measured diameter at breast height (DBH), and measured root diameter and measured DBH] are tested to verify the correlation between the main parameters of the volume model. Lastly, three volume models [unary tree height–volume model (M_1), unary root diameter–volume model (M_2), and binary tree height and root diameter–volume model (M_3)] are built and compared and analyzed through the calculation of the felled tree volume, taking the measured volume as the reference data. The experimental results showed that the correlation coefficient and root mean square error of the three volume models are 0.9093 and 0.1233, 0.9589 and 0.0831, and 0.9796 and 0.0584, respectively. This study demonstrates that by combining UAV visible light remote sensing with artificial intelligence, highly intelligent forest harvesting supervision can be achieved at a much lower cost than traditional field investigation.

*Corresponding author: e-mail: liangdan812345@163.com
https://doi.org/10.18494/SAM3996

ISSN 0914-4935 © MYU K.K.
https://myukk.org/

1. Introduction

Field surveys are the main activity in forest investigation and supervision. They are time-consuming, labor-intensive, and particularly difficult in complex terrain. With the development of unmanned aerial vehicle (UAV) remote sensing technology and the application of artificial intelligence (AI) in the field of image recognition, intelligent methods are increasingly being used in field surveys.(1–6)

In this paper, we report research on the use of UAV remote sensing technology combined with AI for supervising forest cutting. According to forestry laws of the People's Republic of China,(7) a forest cutting quota system specifies the maximum total volume of trees that can be consumed by all kinds of cutting.(8) Forest cutting supervision is an important part of implementing the forest cutting quota system.(9) Effective supervision of the forest cutting volume is the key requirement of forest harvesting supervision,(10) which aims to increase forest stock and preserve the ecological environment of the country. Forest stock refers to the total volume of tree trunks in a certain area.(11) In the regulations for the implementation of the forest law, the number of trees to be felled must not exceed 5% of the total number of trees according to the specified requirements.

Because the cutting process is managed independently by forest operators and because of the lack of tracking of key cutting processes, excessive cutting can easily occur, and it is difficult to find and stop this phenomenon in a timely manner.(12) Traditional field tracking and supervision are not only time-consuming and laborious, but also prone to omissions, making it difficult to accurately supervise tree cutting. In recent years, intensive studies have focused on the calculation of forest stock using UAV remote sensing images based on AI methods. Li *et al.*(13) used high-resolution UAV images and field data of the canopy width to build a model correlating canopy width and diameter at breast height (DBH), which they used to calculate the forest stock volume. Similar work was reported by Zhou *et al.*(14) Moreover, UAV airborne light detection and ranging (LiDAR) is now widely used in forest inventory to provide accurate forest information, which has the advantage of directly measuring the 3D coordinates of the tree canopy.(15,16) Important forest parameters such as the treetop, tree height, canopy width, and DBH can be easily extracted by airborne LiDAR based on the canopy height model.(17,18) However, airborne LiDAR is expensive and cannot be afforded by small organizations. In addition, to the best of our knowledge, the forest stock is calculated at the plot scale in most studies, and less attention has been focused on the forest cutting stock at the scale of individual felled trees.

In this study, Chinese fir, one of the main forestry cutting tree species, is selected as the research object. By UAV oblique photography, raw image data are obtained and further processed into a digital orthophoto map (DOM) and digital surface model (DSM) using the structure from motion (SFM) algorithm for 3D reconstruction.(19,20) Treetops are detected using the local maximum (LM) method based on DSM data before and after the cutting, and the geometric center and root diameter are determined by the circumcircle method based on DOM data. Treetops are matched to the corresponding stump points; then, the tree height is estimated from the elevation difference between the treetop and the stump. Finally, regressions among tree height, root diameter, and DBH pairs are analyzed. Three volume models (unary tree height–volume model, unary root diameter–volume model, and binary tree height and root diameter–volume model) are established. The three volume models are compared and analyzed through the calculation of the felled tree volume, taking the measured volume as the reference data.

2. Materials

2.1 Study area

The study was conducted in Jingning County, Lishui City, Zhejiang Province, China (119°39′50.4″E–119°39′57.60″E, 27°53′52.79″N–27°53′41.99″N). The plot is mainly covered by coniferous and broad-leaved mixed forest with a canopy density of 0.9, a sparse density of 0.82, and elevation between 1045 and 1080 m. The primary tree species are *Cunninghamia lanceolata*, *Pinus massoniana*, *Cryptomeria japonica* var. *sinensis Miquel*, *Gugertree*, and *Ligustrum lucidum*. The study area with a UAV ortho-mosaic of the forest is presented in Fig. 1.

2.2 Image acquisition and processing

We used a DJI Phantom 4 RTK UAV platform (Fig. 2) with a take-off weight of 1.39 kg, GPS/GLONASS/BeiDou satellite systems, and an ultrasonic module to enable precise hovering and detect obstacles ahead. The integrated RGB camera had a 1/2.3″ CMOS sensor with a lens range of 8.8–24 mm and a field of view of 84°, with a 1-inch, 20-megapixel sensor and a dynamic range of nearly 12 stops. This camera system can deliver outstanding image quality in both detailed and dark conditions. For more detailed information about the system, please refer to https://www.dji.com/cn/phantom-4-rtk/info#specs.

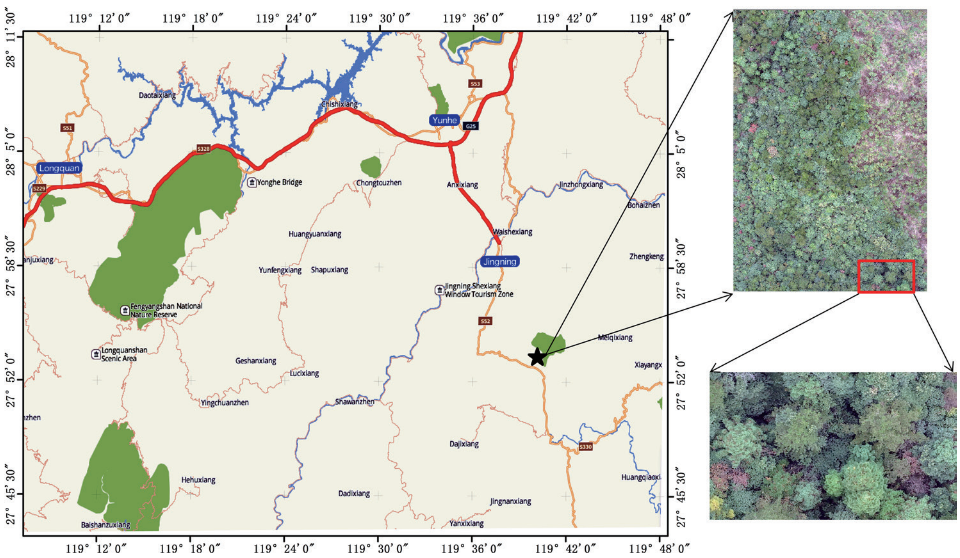

Fig. 1. (Color) Study area and canopy conditions shown in ortho-mosaic.

Fig. 2. (Color online) Phantom 4 UAV.

Table 1
Basic flight parameters.

Technology index	Parameter value
Flight speed	5 m/s
Flight altitude	70 m
Sailing direction overlap percentage	90%
Side overlap percentage	90%

High-resolution UAV images were obtained in February 2021. The basic flight parameters are shown in Table 1. A total of 251 raw images were taken. After pre-processing (incorrect and blurred images were removed and the remaining images were re-exposed to increase brightness), the processed images were used to generate a DOM and DSM by image reconstruction using the SFM algorithm in DJI Terra software.

2.3 Field investigation

An actually cut Chinese fir was identified as the target tree of the experiment (Fig. 3). The target tree was measured at 2 m intervals using the differential quadrature formula for felled trees. To obtain the reference location of the felled trees, a South Galaxy 6 RTK (real-time kinematic) receiver (Guangzhou Nanfang Surveying Instrument Co. Ltd.) with accuracy higher than 3 cm was used to measure the location of the stump of the felled tree. For more detailed information about the South Galaxy 6 RTK, please refer to http://www.southsurvey.com/product-2200.html. The measured volume of the felled tree was calculated as follows:(11)

$$v = l\sum_{i=1}^{n} g_i + \frac{1}{3} g'l', \tag{1}$$

where g_i is the central sectional area of segment i, l is the length of the segment, g' is the basal sectional area of the tip, l' is the tip length, and n is the number of segments.

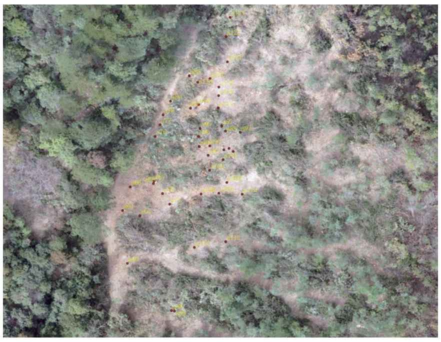

(a)

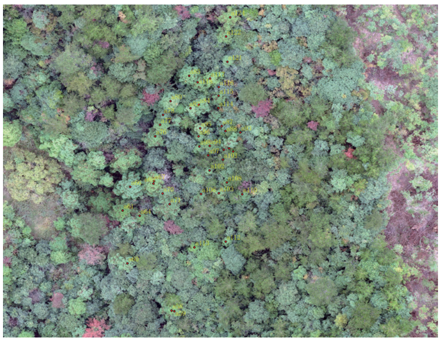

(b)

Fig. 3. (Color) Cutting site: (a) before cutting and (b) after cutting.

3. Methods

3.1 Treetop detection based on LM method

The LM method is the main method used to detect treetops, which is based on the principle that the treetop represents the maximum elevation of the target point in an identification window centered on itself.[21,22] Prior to the implementation of the LM method, to eliminate the interference from other standing trees, a DSM difference image is obtained by subtracting the DSM of the before-cutting data from that of the after-cutting data. Then, the LM method with a circular dynamic window is used to detect treetops. In this study, the window radius was set to 3, 5, 7, and 9 pixels. The results of treetop detection are shown in Fig. 4.

3.2 Tree height estimation

Since tree trunks are not straight, a direct way of calculating the difference between the elevation of the treetop and the stump point will result in a large deviation in the tree height estimation. Thus, we propose a new method for estimating tree height using the 3D coordinates of the treetop and stump point.

The estimated tree height h_{dsm} of the felled tree is calculated as

$$h_{dsm} = \sqrt{(x-x')^2 + (y-y')^2 + (z-z')^2}, \tag{2}$$

where x, y, z are the coordinates of the treetop extracted from the DSM image and x', y', z' are the coordinates of the center point of the stump.

3.3 Root diameter acquisition based on circumcircle method

On the basis of the after-cutting DOM data, the felled tree stump is recognized and the boundary of the tree root pile is delineated in ArcGIS software. The estimated root diameter d_{root} is calculated as follows using the circumcircle method shown in Fig. 5:

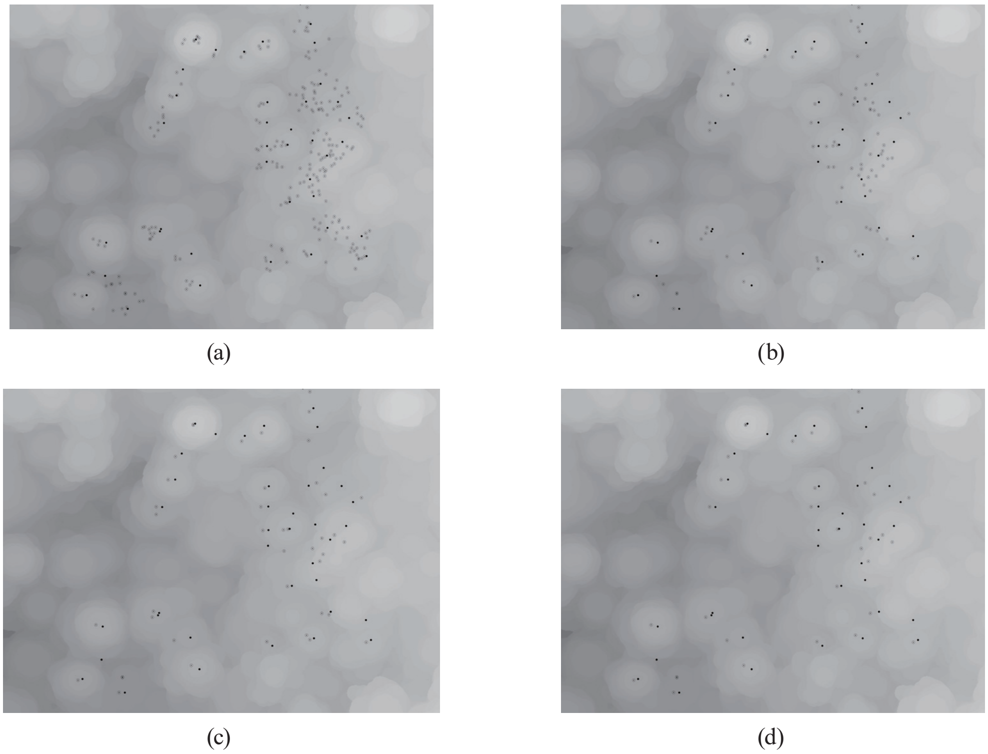

Fig. 4. Treetop maps obtained by LM method: (a) 3 pixels, (b) 5 pixels, (c) 7 pixels, and (d) 9 pixels.

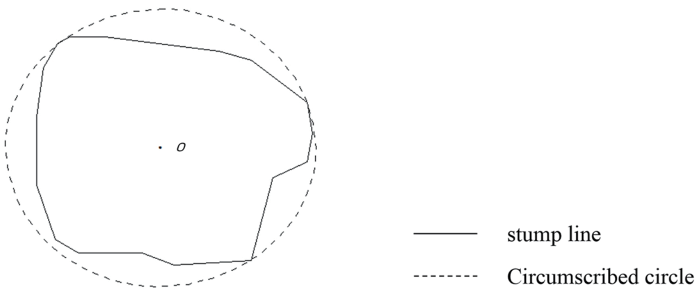

Fig. 5. Diagram of the tree stump center.

$$d_{root} = 2 * \sqrt{\frac{S}{\pi}}, \tag{3}$$

where S is the area of the tree root pile. The center of the circle is taken as the stump position.

4. Results and Discussion

4.1 Result of treetop detection based on LM method

The results of treetop detection using the LM method with different window sizes are shown in Table 2. The window size is the most important factor affecting the accuracy of treetop

Table 2
Results of treetop detection with different window sizes.

Window size /pixels	Tree stumps	Treetops detected	Missing tops	Invalid tops
3	78	454	2	378
5	78	163	5	90
7	78	97	9	28
9	78	74	12	8

detection based on the LM method. It is known that a smaller window size tends to detect invalid treetops because the same tree is detected multiple times, whereas a larger window size makes it easy to miss treetops.(15,22) In our study, we found that when the window size is set to 7 × 7 pixels, the number of extracted treetops is much closer to the real number of target trees than for the 3 × 3, 5 × 5, and 9 × 9 window sizes and the number of invalid vertices is relatively low. Furthermore, by comparing these results with those obtained by manual interpretation, we find that the missing treetops were due to two or more tree stumps being close to each other (10–30 cm apart), making them difficult to distinguish.

4.2 Modeling results of regression between estimated tree height and measured tree height

The regression model (denoted as R_{TH}) of the estimated and measured tree heights based on the measured data of 78 Chinese fir trees in the experimental plot is shown in Fig. 6. It can be seen that the correlation coefficient R^2 of R_{TH} is 0.9023 and $RMSE$ is 0.905. These values indicate that the estimated tree height h_{dsm} has a strong correlation with the measured tree height. The measured value can thus be taken as the true value.

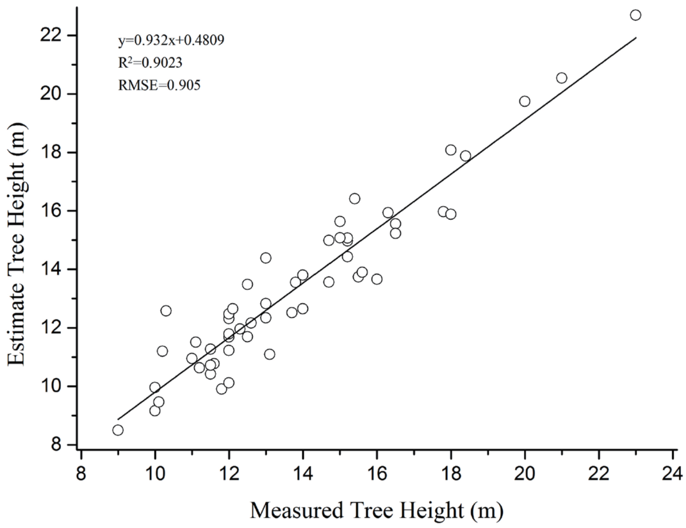

Fig. 6. Linear regression of estimated and measured tree heights.

4.3 Modeling results of fitting between measured tree height and measured DBH

The result of curve fitting between the measured tree height and the measured DBH is shown in Fig. 7. The accuracy of the curve fitting is $R^2 = 0.8122$ and $RMSE = 0.9011$. The regression model $R_{\text{HD-DBH}}$ is obtained [Eq. (4)], from which we estimate the DBH (denoted as d) as

$$d = 5.3947e^{0.095h_{dsm}}, \tag{4}$$

where h_{dsm} is the estimated tree height.

4.4 Modeling results of regression between estimated root diameter and measured DBH

The regression (denoted as $R_{droot\text{-}DBH}$) result of the measured DBH based on the estimated root diameter is plotted in Fig. 8. R^2 for $R_{droot\text{-}DBH}$ is 0.953, which is higher than the correlation coefficient of 0.89 for the tree height and DBH model in Zhou *et al.*,[14] and $RMSE$ is 0.976. This indicates that the measured root diameter has a strong correlation with the true value of the DBH. The fitted DBH (DBH_{root}) is calculated from the estimated root diameter as follows:

$$DBH_{root} = 0.81833306d_{root} + 0.8, \tag{5}$$

where d_{root} is the estimated root diameter obtained from Eq. (3).

4.5 Modeling results of individual tree volume

In forestry, the tree height and DBH are usually used to build a unary or binary volume model to calculate the tree volume.[11] For a felled tree, the tree height and root diameter can be obtained

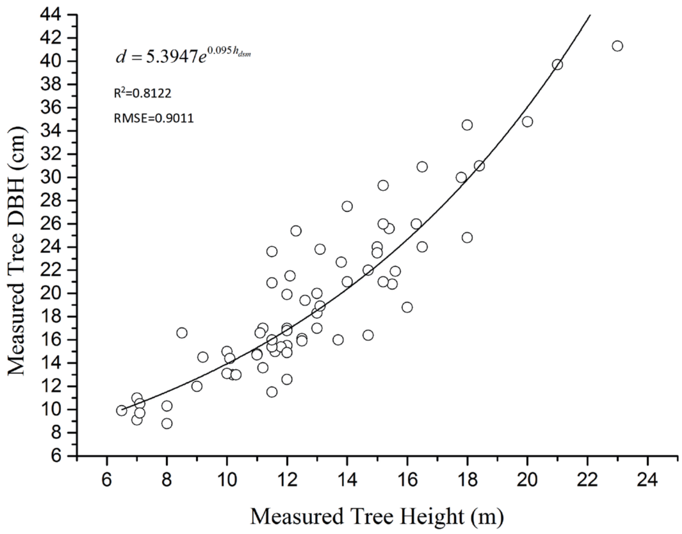

Fig. 7. Curve fitting between measured tree height and measured tree DBH.

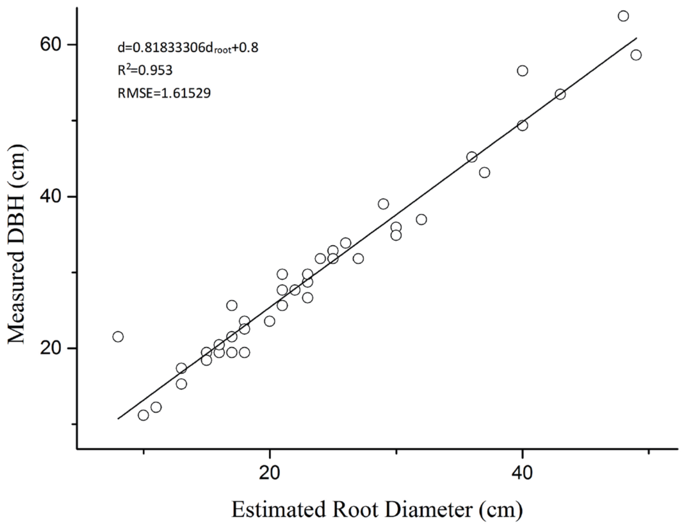

Fig. 8. Regression result of measured DBH and estimated root diameter.

from UAV remote sensing data. In this study, we use the root diameter instead of the DBH to calculate the volume. Among the volume models of the Chinese fir tree in Zhejiang Province,(23,24) the following three volume models (unary tree height–volume model (M_1), unary root diameter–volume model (M_2), and binary tree height and root diameter–volume model [(M_3)] are selected and analyzed:

$$M_1: V = 0.00005806186 * (5.39478e^{0.095*h_{dsm}})^{1.9553351} * h_{dsm}{}^{0.89403304}, \tag{6}$$

$$M_2: V = 0.00005806186 * DBH_{root}{}^{1.9553351} * (119.584 + \frac{-24448.21}{DBH_{root} + 206})^{0.89403304}, \tag{7}$$

$$M_3\text{: } V = 0.00005806186 * DBH_{root}{}^{1.9553351} * h_{dsm}{}^{0.89403304}. \tag{8}$$

As shown in Table 3, a comparative analysis reveals that model M_3 has the highest accuracy, with R^2 of 0.9796 and *RMSE* of 0.0584. Secondly, volume model M_2 has R^2 of 0.9589 and *RMSE* of 0.0831; the accuracy of model M_1 is the lowest with R^2 of 0.9093 and *RMSE* of 0.1233. The three volume models are compared and analyzed through the calculation of the felled tree volume, taking the measured volume as the reference data. Figure 9 clearly shows that the results

Table 3
Accuracy of the three volume models.

Model	R^2	*RMSE*
M_1	0.9093	0.1233
M_2	0.9589	0.0831
M_3	0.9796	0.0584

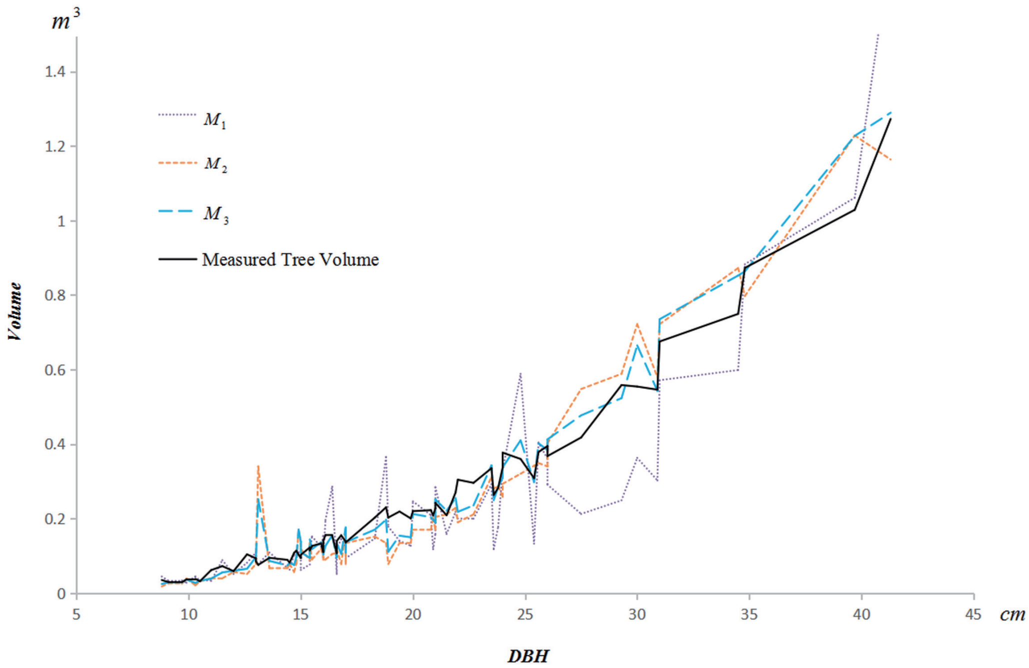

Fig. 9. (Color) Comparison between calculated and measured values.

of the model calculations using the root diameter (M_2 and M_3) are close to the actual measurement data.

In our study, the correlation coefficient R^2 of the root diameter and DBH model is 0.953 (shown in Fig. 8), which is higher than that of 0.89 for the tree height and DBH model in Zhou *et al.*(14) The accuracy of after-cutting volume estimation obtained from the binary volume model is 0.9796, which is 6.69 points higher than that of 0.91 for the tree height–volume model of Zhou *et al.*(14) The experimental results reveal that 1) the tree height can be obtained from UAV image data with high accuracy and 2) the root diameter can be used instead of the DBH to calculate felled tree volumes in practice.

5. Conclusion

AI technology is widely used in the forestry field, with the extraction of information from UAV aerial images playing an important role in forest resource management, forest disease monitoring, and so forth. In this paper, a workflow for forest cutting quota management is proposed. Firstly, two aerial flights of a UAV are implemented to obtain oblique images (i.e., before and after cutting), The raw images are processed in DJI Terra software to obtain DOM and DSM data. Secondly, based on the before- and after-cutting DSM data, treetops are extracted using the LM method. Treetops are matched to the corresponding stump points, then the tree heights of the felled trees are estimated. Using the after-cutting DOM data, the root diameter and the geometric center of the felled tree are determined by the circumcircle method. Thirdly, three regression models (estimated tree height and measured tree height, measured tree height and measured DBH, measured root diameter and measured DBH) are tested to verify the correlation between these main parameters for volume estimation. Lastly, three volume models (M_1, M_2, M_3) are built and analyzed through the calculation of the felled tree volume, taking the measured volume as the reference data. The experimental results show that the correlation coefficient R^2 and root mean square error RMSE of the three volume models are 0.9093 and 0.1233, 0.9589 and 0.0831, and 0.9796 and 0.0584, respectively. This study demonstrates that by combining UAV visible light remote sensing with AI, highly intelligent forest cutting quota management can be achieved at a much lower cost than that of traditional field investigation. Note that the source of the error from field measurement and imagery data was ignored but will studied in depth in the future. Moreover, to automatically acquire the tree height and root diameter with high accuracy, our future research will be focused on treetop detection from DSM data and felled stump delineation from DOM data using more intelligent and automated algorithms.

Acknowledgments

This study was sponsored by a science project of Jingning She Autonomous County (grant no. 2020A19) and the Zhejiang Agriculture and Forestry University Research Development Fund Project (grant no. 2022LFR039).

References

1 Q. W. Liu, S. M. Li, Z. Y. Li, L. Y. Fu, and K. L. Hu: Scientia Silvae Sinicae **53** (2017) 134. https://doi.org/10.11707/j.1001-7488.20170714
2 G. L. Gao, Z. B. Xin, G. D. Ding, C. C. Li, J. Y. Zhang, W. J. Liang, Y. An, Y. He, M. Xiao, and W. Y. Li: Acta Ecol. Sinica **33** (2013) 1675. https://doi.org/10.5846/stxb201112011838
3 J. Q. Shi, Z. K. Feng, and J. C. Liu: Trans. Chin. Soc. Agric. Eng. **33** (2017) 82. https://doi.org/10.11975/j.issn.1002-6819.2017.11.011
4 J. Guerra-Hernández, E. González-Ferreiro, A. Sarmento, João. Silva, A. Nunes, A. C. Correia, L. Fontes, M. Tomé, and R. Díaz-Varela: For. Syst. **25** (2016). https://doi.org/10.5424/fs/2016252-08895
5 J. C. Lv, Z. X. Wang, Y. Q. Yang, Y. B. Qu, Q. Y. Ma, and S. M. Zhu: Xinjiang Agric. Sci. **58** (2021) 1838. https://doi.org/10.6048/j.issn.1001-4330.2021.10.009
6 P. Stefano, B. Johannes, and A. Rasmus: Remote Sens. **12** (2020) 1245. https://doi.org/10.3390/rs12081245
7 Law of the People's Republic of China on Forest (China Forestry Publishing House, Beijing, 2019).
8 S. X. Xie: State Acad. For. Admin. J. **2** (2015) 54. https://doi.org/10.3969/j.issn.2095-2880.2015.02.012
9 J. X. Ouyang, Y. H. Li, X. Q. Wu, and J. Cao: For. Resour. Manage. **5** (2017) 4. https://doi.org/10.13466/j.cnki.lyzygl.2017.05.002
10 J. Z. Meng, Y. Q. Shen, and Y. Q. Mei: Issues For. Econ. **36** (2016) 501. https://doi.org/10.16832/j.cnki.1005-9709.2016.06.004
11 X. Y. Meng: Tree Surveying (China Forestry Publishing House, Beijing, 2006).
12 H. Z. Wang: For. Resour. Manage. **16** (2020) 15. https://doi.org/10.13466/j.cnki.lyzygl.2020.04.003
13 Y. Li, X. R. Wen, G. H. She, and G. Z. Lin: For. Res. **30** (2017) 653. https://doi.org/10.13275/j.cnki.lykxyj.2017.04.017
14 X. C. Zhou, Y. He, H. Y. Huang, and X. Q. Xu: Sci. Silvae Sinicae **55** (2019) 117. https://doi.org/10.11707/j.1001-7488.20191113
15 S. Y. Chen, D. Liang, B. B. Ying, W. J. Zhu, G. M. Zhou, and Y. X. Wang: Int. J. Remote Sens. **42** (2021) 106. https://doi.org/10.1080/01431161.2020.1809024
16 L. F. Zhou, R. Meng, Y. Y. Tan, Z. G. Lv, Y. T. Zhao, B. Y. Xu, and F. Zhao: Urban For. Urban Greening **69** (2022). https://doi.org/10.1016/j.ufug.2022.127489
17 H. L. Liu, X. L. Zhang, Y. Zhang, Y. F. Zhu, H. Liu, and L. Y. Wang: Laser Optoelectron. Prog. **55** (2018) 40. https://doi.org/10.3788/LOP55.082805
18 P. Li, Z. K. Feng, and J. Y. Su: Sci. Surv. Mapp. **47** (2022) 151. https://doi.org/10.16251/j.cnki.1009-2307.2022.02.020

19 Y. W. Sun and W. S. Lin: J. Northwest For. Univ. **35** (2020) 180. https://doi.org/10.3969/j.issn.1001-7461.2020.05.28

20 Q. Y. Yang, Z. Y. Dong, Z. Y. Ma, Y. Wu, Q. Cui, and H. Lu: Trans. Chin. Soc. Agric. Mach. **51** (2020) 181. https://doi.org/10.3969/j.issn.1000-2324.2021.02.012

21 K. Stuart, G. M. S. Tanja, M. Jan-Peter, and G. Klaus: Remote Sens. **11** (2019) 758. https://doi.org/10.3390/rs11070758

22 K. Liu, X. Shen, L. Cao, G. B. Wang, and F. L. Cao: ISPRS J. Photogramm. Remote Sens. **146** (2018) 465. https://doi.org/10.1016/j.isprsjprs.2018.11.001

23 Z. Z. Mao: J. Zhe Jiang For. Coll. **5** (1988) 75.

24 A. X. Liu, S. F. Gong, and Y. H. Sun: East Chin. For. Manage. **6** (1992) 12.

About the Authors

Jian-hua Hou received her B.S. degree in cartography and geographic information engineering from LuDong University in 2011 and her M.S. degree in forest management from Zhejiang A&F University in 2014. She is a forestry engineer with the Natural Resources and Planning Bureau of Jingning She Autonomous County. Her research interests are forest ecology and forest resource management. (644124419@qq.com)

Jian-ying Wang received his B.S. degree in geographic information systems from Huazhong Agricultural University in 2011. He is a senior information systems project manager of the Natural Resources and Planning Bureau of Jingning She Autonomous County. His research interests are the spatial data management and information management of natural resources. (379342263@qq.com)

Xue-xin Ma received his M.S. degree in agricultural informatization from Zhejiang A&F University in 2019. He is a natural resources engineer with the Natural Resources and Planning Bureau of Jingning She Autonomous County. His research interests include agricultural and forestry informatization. (457283836@qq.com)

Dan Liang received her B.S. degree in surveying and mapping engineering from Southwest Jiaotong University in 2006 and her Ph.D. degree in cartography and geographic information engineering from Tongji University in 2012. She is a lecturer with Zhejiang A&F University. Her research interests are UAV forestry remote sensing and map matching. (liangdan812345@163.com)